Asian Journal of Chemistry; Vol. 26, No. 24 (2014), 8543-8546

ASIAN JOURNAL OF CHEMISTRY

http://dx.doi.org/10.14233/ajchem.2014.18322

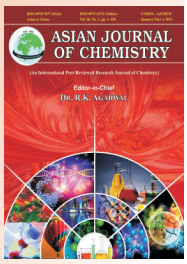

Synthesis of Cl Doped g-C_3N_4 with Enhanced Photocatalytic Activity Under Visible Light

J. WAN[1], S.Z. HU[2,*], F.Y. LI[2], Z.P. FAN[2], F. WANG[3] and J. ZHANG[4]

[1]School of Experimental Education, Liaoning Shihua University, Fushun 113001, P.R. China
[2]Institute of Eco-environmental Sciences, Liaoning Shihua University, Fushun 113001, P.R. China
[3]School of Environmental and Biological Engineering, Liaoning Shihua University, Fushun 113001, P.R. China
[4]Liaoning Key Laboratory of Petroleum & Chemical Industry, Liaoning Shihua University, Fushun 113001, PR China

*Corresponding author: Tel: +86 24 23847473; E-mail: jiewanlnpu@163.com

Received: 13 June 2014; *Accepted*: 15 September 2014; *Published online*: 1 December 2014; AJC-16399

Cl-doped g-C_3N_4 was prepared by a simple method using dicyandiamide and NH_4Cl as precursors. X-ray diffraction, UV-visible spectroscopy, Fourier transform infrared spectra, scanning electron microscope and photoluminescence were used to characterize the prepared catalysts. The results indicated that the introduction of Cl decreased the band gap energy and increased the separation efficiency of photogenerated electrons and holes. The activities of Cl doped g-C_3N_4 catalysts were tested in the photocatalytic degradation of Rhodamine-B under visible light. The rate constant of Cl doped g-C_3N_4 was 3.5 times higher than that of neat g-C_3N_4. The possible mechanism was proposed.

Keywords: g-C_3N_4, Chlorine doping, Photocatalysis, Visible light, Rhodamine-B, Degradation.

INTRODUCTION

The growing concerns about environmental and energy crises have stimulated intense research on solar energy utilization[1]. In the field of elimination of organic pollutants, photocatalysis has emerged as one of the most promising technologies. Nevertheless, wide band gap energy and low quantum efficiency are still the "bottleneck" of the photocatalyst to meet the requirement of practical applications. For example, the most common TiO_2 is not an ideal photocatalyst because it performs rather poorly ability to absorb visible light. As a result, it is an urgent issue to search for efficient visible-light-driven photocatalyst. Modified TiO_2 photocatalysts have been developed to resolve this problem[2-7]. However, it still remains a challenge to design photocatalysts that are abundant and facile preparation besides high visible-light efficiency.

In search for stable visible-light-driven photocatalyst, graphitic carbon nitride, g-C_3N_4, has recently attracted a great deal of interest in photocatalytic applications. The heptazine ring structure and high degree of condensation make metal-free g-C_3N_4 possess many advantages such as good chemical stability as well as an appealing electronic structure with a medium-band gap (2.7 eV). In addition, g-C_3N_4 is abundant and easily-synthesized *via* one-step polymerization of the low-cost materials.

Recently, halogen atoms were used to modify g-C_3N_4 catalysts. Wang *et al.*[8] prepared F doped g-C_3N_4 catalysts using NH_4F as raw material. Zhang *et al.*[9] prepared iodine modified g-C_3N_4 semiconductors as visible light photocatalysts for hydrogen evolution. In this work, Cl doped g-C_3N_4 semiconductors was prepared using NH_4Cl as raw material. The prepared catalysts were tested in the photocatalytic degradation of Rhodamine-B under visible light. A possible mechanism for the photocatalysis was proposed.

EXPERIMENTAL

In a typical experiment, 3 g dicyandiamide was dissolved into 15 mL deionized water under stirring. Then 0.1, 0.5 and 1 g NH_4Cl was added. The obtained solution was heated to 100 °C under stirring to remove the water. The solid product was dry at 100 °C in oven, followed by milling and annealing at 520 °C for 2 h (at a rate of 5 °C min^{-1}). The prepared catalyst was denoted as Cl(x)-CN, where x stands for the mass of NH_4Cl. For comparison, g-C_3N_4 was prepared following the same procedure as in the synthesis of Cl(x)-CN but in the absence of NH_4Cl.

XRD patterns of the prepared TiO_2 samples were recorded on a Rigaku D/max-2400 instrument using CuK_α radiation (λ = 1.54 Å). UV-visible spectroscopy measurement was carried out on a JASCO V-550 model UV-visible spectrophotometer, using $BaSO_4$ as the reflectance sample. Fourier transform infrared spectra (FT-IR) were obtained on a Nicolet 20DXB FT-IR spectrometer. The morphology of prepared catalyst was

observed by using a scanning electron microscope (SEM, JSM 5600LV, JEOL Ltd.). Photoluminescence spectra were measured at room temperature with a fluorospectrophotometer (FP-6300) using an Xe lamp as excitation source.

Rhodamine-B (RhB) was selected as model compound to evaluate the photocatalytic performance of the prepared *g*-C_3N_4 and Cl(x)-CN catalysts in an aqueous solution under visible light irradiation. 0.05 g catalyst were dispersed in 200 mL aqueous solution of Rhodamine-B (10 ppm) in an ultrasound generator for 10 min. The suspension was transferred into a self-designed glass reactor and stirred for 0.5 h in darkness to achieve the adsorption equilibrium. In the photoreaction under visible light irradiation, the suspension was exposed to a 250 W high-pressure sodium lamp with main emission in the range of 400-800 nm and air was bubbled at 130 mL/min through the solution. The UV light portion of sodium lamp was filtered by 0.5 M $NaNO_2$ solution[10]. All runs were conducted at ambient pressure and 30 °C. At given time intervals, 4 mL suspension was taken and immediately centrifuged to separate the liquid samples from the solid catalyst. The concentrations of Rhodamine-B before and after reaction were measured by means of a UV-visible spectrophotometer at a wavelength of 550 nm.

RESULTS AND DISCUSSION

XRD analysis is used to investigate the phase structure of prepared photocatalysts (Fig. 1). The typical (002) interlayer-stacking peak at 27.3° corresponds to an interlayer distance of d = 0.32 nm for *g*-C_3N_4, while the peak at 13.1° represents in-plane structural packing motif (100) with a period of 0.675 nm[11,12]. No peak for chlorine species was observed in all the Cl-doped *g*-C_3N_4 materials. Besides, compared with *g*-C_3N_4, a obvious shift toward a higher 2θ value is observed for Cl(x)-CN catalysts. This is probably due to that Cl atoms doped into *g*-C_3N_4 lattice which caused the lattice distortion. Such lattice distortion could cause many crystal lattice defect which is favorable for the photocatalytic performance.

FT-IR spectra (Fig. 2) can provide plentiful structural information concerning of synthesized *g*-C_3N_4 and Cl(0.5)-CN. For *g*-C_3N_4, a series of peaks in the range from 1600 to 1200 cm^{-1}

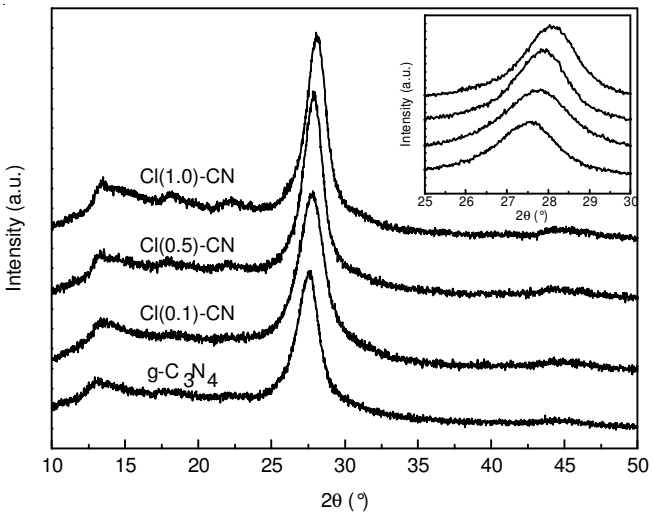

Fig. 1. XRD patterns of the prepared catalysts

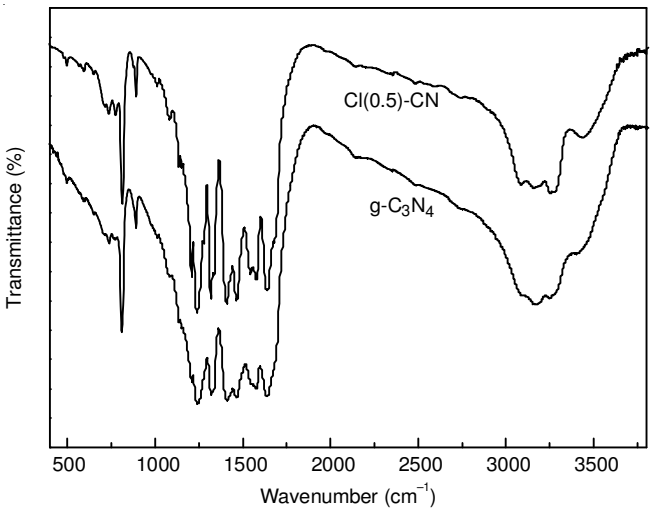

Fig. 2. FT-IR spectra of prepared catalysts

are attributed to the typical stretching modes of CN heterocycles, while the sharp peak located at 810 cm^{-1} is assigned to the bending vibration of heptazine rings, which indicating the synthesized *g*-C_3N_4 is composed of heptazine units. The broad absorption band around 3200 cm^{-1} is originated from the stretching vibration of N-H bond, associated with uncondensed amino groups[13,14]. For Cl(0.5)-CN, all the characteristic vibrational peaks of *g*-C_3N_4 are observed, suggesting that the structure of *g*-C_3N_4 is not changed after Cl doping. The vibrations of Cl-related group were not observed in their investigation. This is probably due to the low Cl content or its vibration was overlapped by that of C-N bond.

Fig. 3 shows the UV-visible spectra which test the light absorption property of as-prepared *g*-C_3N_4 and Cl(x)-CN catalysts. Pure *g*-C_3N_4 shows a typical semiconductor absorption, originating from charge transfer response of *g*-C_3N_4 from the valence band populated by N 2p orbitals to the conduction band formed by C 2p orbitals[11]. For Cl(x)-CN, the slight red shifts of absorption band were observed with increasing the Cl content, indicating Cl doped into *g*-C_3N_4 lattice could affect its electronic structure, thus changes the optical property of *g*-C_3N_4 and decreased the band gap energy. Zhang *et al.*[9] prepared I doped *g*-C_3N_4 catalysts and found the similar

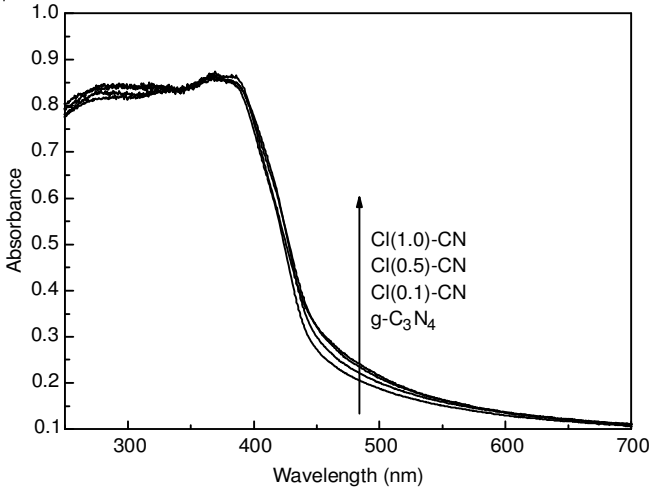

Fig. 3. UV-visible diffuse reflectance spectra of prepared catalysts

phenomenon[9]. The band gap energy, which is calculated according to the method of Oregan and Gratzel, is 2.72 eV for g-C_3N_4. This is consistent with the previous results[15-17]. In the case of Cl(0.1)-CN, Cl(0.5)-CN and Cl(1.0)-CN, this value decreased to 2.70, 2.68 and 2.68 eV. Such decreased band gap energy of catalysts is favorable for adsorption more visible light leading to the enhanced photocatalytic performance.

The morphology of prepared g-C_3N_4 based catalysts is investigated by SEM. Fig. 4 shows the SEM images of g-C_3N_4 and Cl(0.5)-CN. All the catalysts exhibit layered structure, similar to its analogue graphite. No obvious difference was shown two SEM images indicated that Cl doping did not influence the morphology of prepared g-C_3N_4.

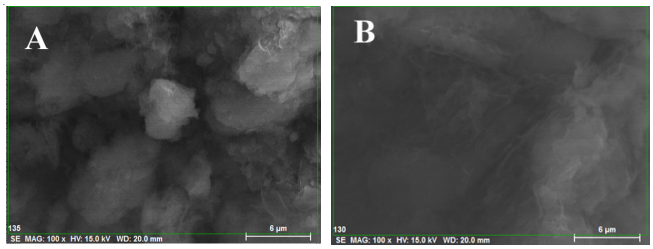

Fig. 4. SEM images of g-C_3N_4 (A) and Cl(0.5)-CN (B)

Fig. 5 shows the room temperature photoluminescence spectra of g-C_3N_4 and Cl(x)-CN under the excitation wavelength of 320 nm. For g-C_3N_4, the broad photoluminescence band is around 465 nm, which can be attributed to the band-band photoluminescence phenomenon with the energy of light approximately equal to the band gap of g-C_3N_4 calculated by UV-visible spectra[18]. Such band-band photoluminescence signal is attributed to excitonic photoluminescence, which mainly results from the n-π^* electronic transitions involving lone pairs of nitrogen atoms in g-C_3N_4[19]. In the case of Cl doped g-C_3N_4, the shape of the curves is similar to that of g-C_3N_4, whereas the peak intensities significantly decrease. Considering that the photoluminescence emission results from the free charge carrier recombination, the decreased peak intensity indicates that Cl doped g-C_3N_4 exhibits lower electrons-holes recombination rate compared with g-C_3N_4. This is probably due to that Cl doping cause the formation of crystal lattice defect which affect its electronic structure. Therefore,

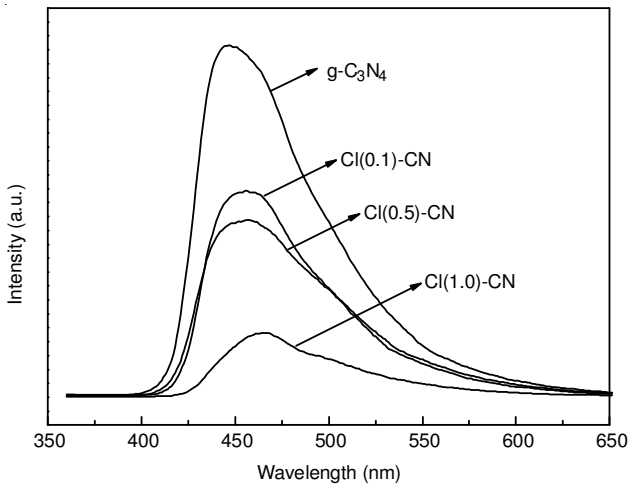

Fig. 5. Photoluminescence spectra of prepared catalysts

the dispersion of the contour distribution of HOMO and LUMO could be increased, which improves the carrier mobility[20]. The noncoplanar HOMO and LUMO favors the separation of photogenerated e^-/h^+ pairs and thus decreases the recombination rate.

The photocatalytic performances of g-C_3N_4 based catalysts in the degradation of Rhodamine-B under visible light irradiation were shown in Fig. 6. Control experiment results indicated that the degradation performance of Rhodamine-B can be ignored in the absence of either irradiation or photocatalyst, indicating that Rhodamine-B was degraded *via* photocatalytic process. 50 % Rhodamine-B was degraded over g-C_3N_4 in 120 min. Cl(x)-CN showed clearly higher activities than that of g-C_3N_4. This increased photocatalytic performance should be due to the synergistic effect of decreased band gap energy and reduced recombination rate of photogenerated electrons/holes pairs, which caused by Cl doping. Cl(0.5)-CN exhibited the highest activity, more than 90 % Rhodamine-B was degraded in 120 min. The reaction rate constant k was obtained by assuming that the reaction followed first order kinetics[21]. In a batch reactor, the performance equation is as follows: $-\ln(C/C_0) = kt$ where C_0 and C represent the concentrations of Rhodamine-B dye before and after photocatalytic degradation, respectively. If a linear relationship is established when $-\ln(C/C_0)$ is plotted against t (reaction time), the rate constant k can be obtained from the slope of the line. The calculated results indicated that the rate constant k was 0.0112, 0.0253, 0.0369 and 0.0302 min^{-1} for g-C_3N_4, Cl(0.1)-CN, Cl(0.5)-CN and Cl(1.0)-CN, respectively. Cl(0.5)-CN exhibited the highest rate constant which is 3.5 times higher than that of g-C_3N_4. This increased photocatalytic performance should be attributed to the synergistic effect of decreased band gap energy which utilize visible light more efficiently and improved electrons-holes separation efficiency.

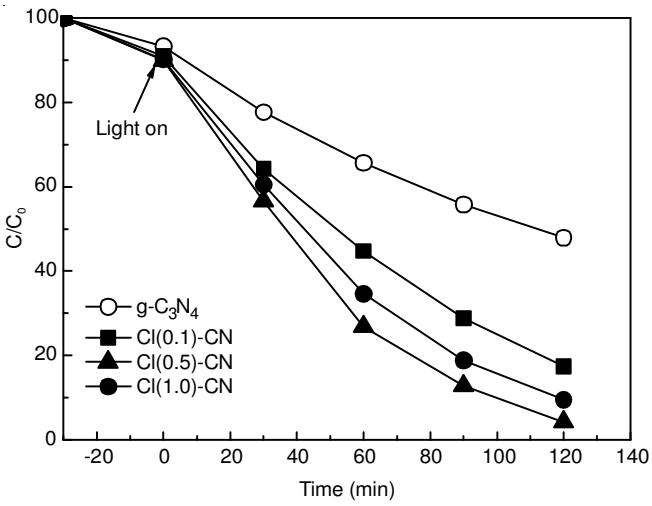

Fig. 6. Photocatalytic performance of degradation of Rhodamine-B over prepared catalysts under visible light

Conclusion

Cl-doped g-C_3N_4 was prepared by a simple method using dicyandiamide and NH_4Cl as precursors. The results indicated that the Cl atoms doped into g-C_3N_4 lattice caused the lattice distortion, which decreased the band gap energy and increased

the separation efficiency of photogenerated electrons and holes. The activities of Rhodamine-B degradation over Cl doped g-C_3N_4 catalysts were much higher than that of neat g-C_3N_4. The rate constant of Cl doped g-C_3N_4 was 3.5 times higher than that of neat g-C_3N_4.

REFERENCES

1. C.C. Chen, W.H. Ma and J.C. Zhao, *Chem. Soc. Rev*., **39**, 4206 (2010).
2. M.L. de Souza and P. Corio, *Appl. Catal. B*, **136-137**, 325 (2013).
3. W.D. Shi, J.Q. Shi, S. Yu and P. Liu, *Appl. Catal. B*, **138-139**, 184 (2013).
4. D.G. Wang, H.F. Jiang, X. Zong, Q. Xu, Y. Ma, G.L. Li and C. Li, *Chem. Eur. J.*, **17**, 1275 (2011).
5. Y.N. Guo, L. Chen, X. Yang, F.Y. Ma, S.Q. Zhang, Y.X. Yang, Y.H. Guo and X. Yuan, *RSC Adv*., **2**, 4656 (2012).
6. B. Siritanaratkul, K. Maeda, T. Hisatomi and K. Domen, *ChemSusChem*, **4**, 74 (2011).
7. J.G. Hou, Z. Wang, W.B. Kan, S.Q. Jiao, H.M. Zhu and R.V. Kumar, *J. Mater. Chem*., **22**, 7291 (2012).
8. Y. Wang, Y. Di, M. Antonietti, H.R. Li, X.F. Chen and X.C. Wang, *Chem. Mater*., **22**, 5119 (2010).
9. G.G. Zhang, M.W. Zhang, X.X. Ye, X.Q. Qiu, S. Lin and X.C. Wang, *Adv. Mater*., **26**, 805 (2014).
10. F.B. Li, X.Z. Li, M.F. Hou, K.W. Cheah and W.C.H. Choy, *Appl. Catal*., **285**, 181 (2005).
11. X. Wang, K. Maeda, A. Thomas, K. Takanabe, G. Xin, J.M. Carlsson, K. Domen and M. Antonietti, *Nat. Mater*., **8**, 76 (2009).
12. Y. Wang, X.C. Wang and M. Antonietti, *Angew. Chem. Int. Ed*., **51**, 68 (2012).
13. S.C. Yan, Z.S. Li and Z.G. Zou, *Langmuir*, **25**, 10397 (2009).
14. S.Z. Hu, L. Ma, J.G. You, F.Y. Li, Z.P. Fan, F. Wang, D. Liu and J.Z. Gui, *RSC Adv*., **4**, 21657 (2014).
15. H.J. Yan and H.X. Yang, *J. Alloys Comp*., **509**, L26 (2011).
16. B. Oregan and M. Gratzel, *Nature*, **353**, 737 (1991).
17. X.C. Wang, S. Blechert and M. Antonietti, *ACS Catal*., **2**, 1596 (2012).
18. L. Ge and C. Han, *Appl. Catal. B*, **117-118**, 268 (2012).
19. V.N. Khabashesku, J.L. Zimmerman and J.L. Margrave, *Chem. Mater*., **12**, 3264 (2000).
20. X.G. Ma, Y.H. Lv, J. Xu, Y.F. Liu, R.Q. Zhang and Y.F. Zhu, *J. Phys. Chem. C*, **116**, 23485 (2012).
21. X.Y. Li, D.S. Wang, G.X. Cheng, Q.Z. Luo, J. An and Y.H. Wang, *Appl. Catal. B*, **81**, 267 (2008).